

Electronic Supplementary Information

Complete Ultrafast Charge Carrier Dynamics in Photoexcited All-Inorganic Perovskite Nanocrystals (CsPbX_3)

Navendu Mondal and Anunay Samanta*

School of Chemistry, University of Hyderabad, Hyderabad 500 046, India

*Corresponding author: anunay@uohyd.ac.in

List of Contents

1. Figure S1. TEM images of CsPbBr_2I , $\text{CsPbBr}_{1.5}\text{I}_{1.5}$ and CsPbI_3 NCs
2. Figure S2. PL decay profiles of all the NCs
3. Figure S3. TA spectrum of CsPbBr_3 NCs at 480 nm excitation
4. Figure S4. TA spectrum of CsPbI_3 NCs at 545 nm excitation.
5. Figure S5. TA spectrum of CsPbBr_2I and $\text{CsPbBr}_{1.5}\text{I}_{1.5}$ at 350 nm excitation.
6. Figure S6. Decay associated spectrum of CsPbBr_2I and $\text{CsPbBr}_{1.5}\text{I}_{1.5}$ at 350 nm excitation
7. Figure S7. Decay associated spectrum of CsPbBr_2I and $\text{CsPbBr}_{1.5}\text{I}_{1.5}$ at 500 and 530 nm excitations, respectively.
8. Figure S8. Time-resolved PL spectra of CsPbBr_3 NCs
9. Figure S9. Up-converted PL decay profiles of CsPbBr_2I and $\text{CsPbBr}_{1.5}\text{I}_{1.5}$
10. Figure S10 and S11. PL spectra and decay profiles of CsPbBr_3 NCs as a function of concentration of OV
11. Table S1. PL decay parameters of all the NCs
12. Table S2. PL decay parameters of CsPbBr_3 NCs in absence and presence of OV
13. Table S3. Up-converted PL decay parameters of CsPbBr_3 NCs
14. Table S4. Up-converted PL decay parameters of CsPbBr_3 NCs in absence and presence of OV
15. Table S5 and S6. Up-converted PL decay parameters of CsPbBr_2I and $\text{CsPbBr}_{1.5}\text{I}_{1.5}$ NCs

Samples for transmission electron microscope (TEM) measurements were prepared by placing a drop of toluene solution of the NCs on carbon coated copper grids. Size and shape of the NCs were examined by Tecnai G2 FE1 F12 transmission electron microscope at an accelerating voltage of 200 kV.

Ultrafast transient absorption technique. The set-up consisted of a mode-locked Ti:sapphire seed laser (Mai Tai, Spectra Physics) operating at 80 MHz repetition rate with an output centering at 800 nm, which was directed to a Ti:sapphire regenerative amplifier (Spitfire ace, Spectra Physics). A high power Q-switched laser (Empower, Spectra Physics) was used for pumping the amplifier. The amplified output of 800 nm (4.2 W) operating at 1 KHz repetition rate was divided into two parts, major part of the beam (3 W) was directed towards optical parametric amplifier (Topas-prime, Spectra Physics) to generate a range of excitation wavelengths used here. The rest part of the amplified beam was passed through an optical delay line of 4 ns followed by a CaF₂ crystal to generate white light continuum. The white light was passed through a beam splitter to generate a signal and reference beams and was directed to the detector (photodiode array) through fibre-coupling unit to record the pump-induced changes at different delay times of the probe beam. All measurements were performed under very low excitation densities (2-4 $\mu\text{J}/\text{cm}^2$) to avoid any non-linear interaction. All spectra presented here were chirp-corrected and the instrumental resolution was ~ 120 fs. All TA measurements were performed up to 3 ns delay time window.

Time-resolved photoluminescence (PL) technique.

To understand the PL dynamics in ultrafast time-scale (<50-60 ps) we employed PL up-conversion technique in which PL of the sample was up-converted by mixing with another time-delayed laser pulse using a sum-frequency generating crystal. The mode-locked Ti:sapphire laser (Mai Tai) with a centre wavelength of 800 nm was directed to up-conversion spectrometer (FOG 100, CDP systems, Russia), where it was converted to 400 nm using a second-harmonic generating BBO crystal. The output was passed through a dichroic mirror, which reflected the 400 nm (excitation light) and transmitted 800 nm. The 800 nm laser beam, served as gate beam, was passed through an optical delay line (4 ns) and finally PL from the sample and gate beam were mixed in a sum frequency generating crystal (BBO) to produce the up-converted PL. The up-converted beam was finally directed to the photomultiplier tube through a monochromator. All measurements were performed under very low excitation regime (0.016 $\mu\text{J}/\text{cm}^2$) to rule out any contributions due to non-linear processes. The instrumental resolution was found to be ~ 180 -200 fs.

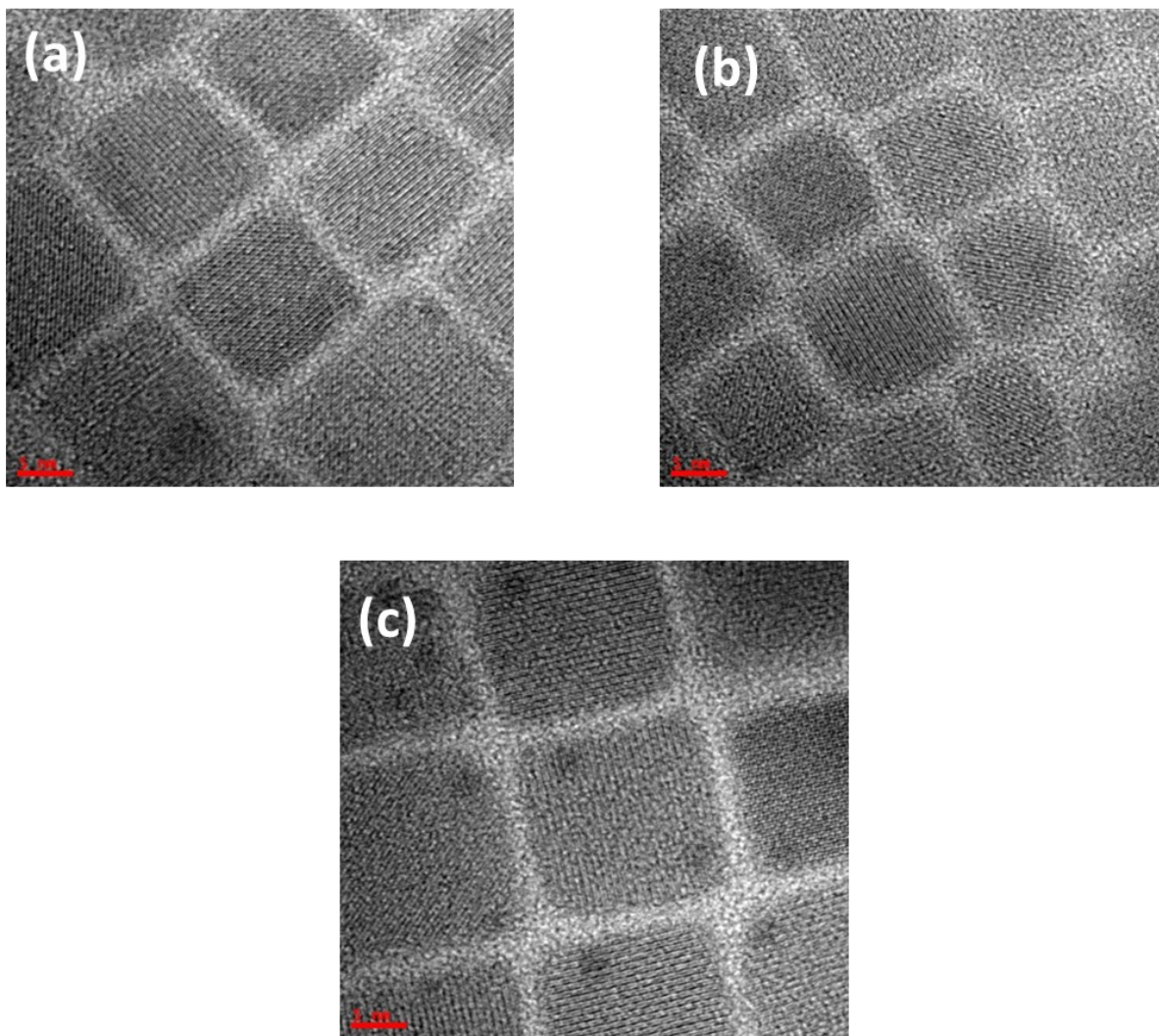


Figure S1. TEM images of cubic (a) CsPbBr_2I (b) $\text{CsPbBr}_{1.5}\text{I}_{1.5}$ and (c) CsPbI_3 NCs. Scale bar shown here is 5 nm.

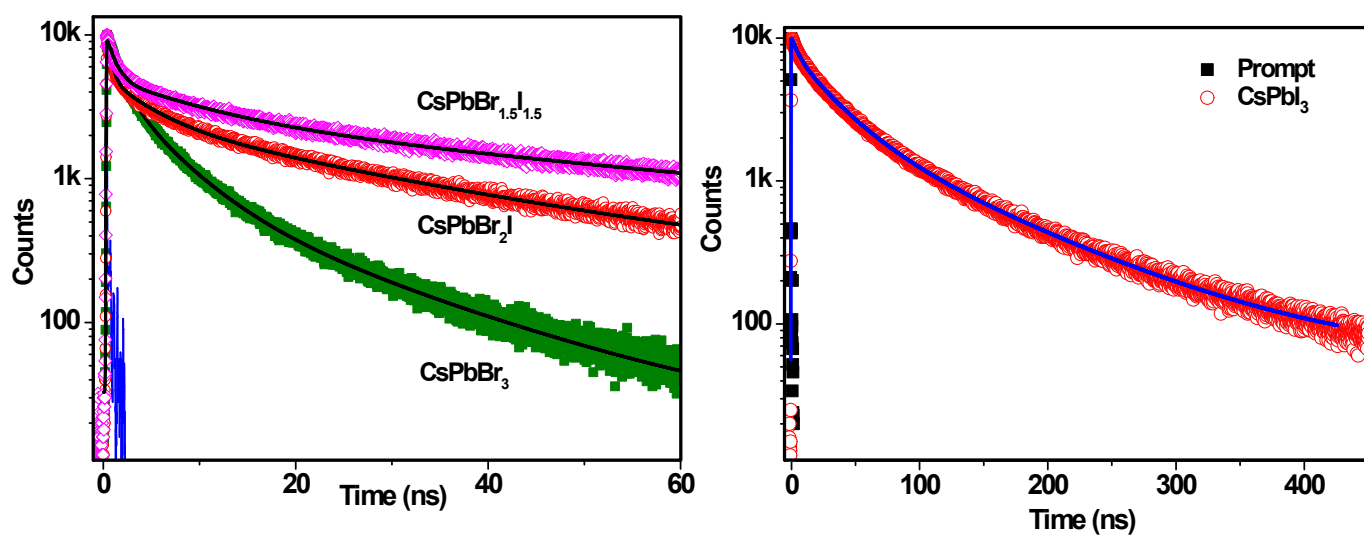


Figure S2. PL decay profiles of all the four NCs monitored at their respective PL maximum. CsPbI₃ decay profiles have recorded at longer time windows as it hardly decays within 100 ns window.

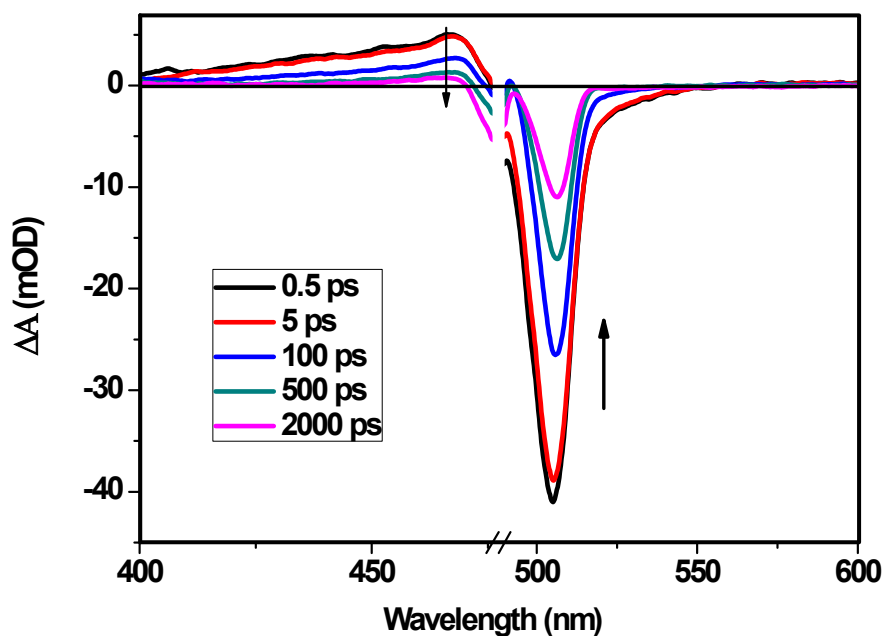


Figure S3. TA spectrum of CsPbBr₃ NCs recorded after (near band-edge) excitation at 480 nm.

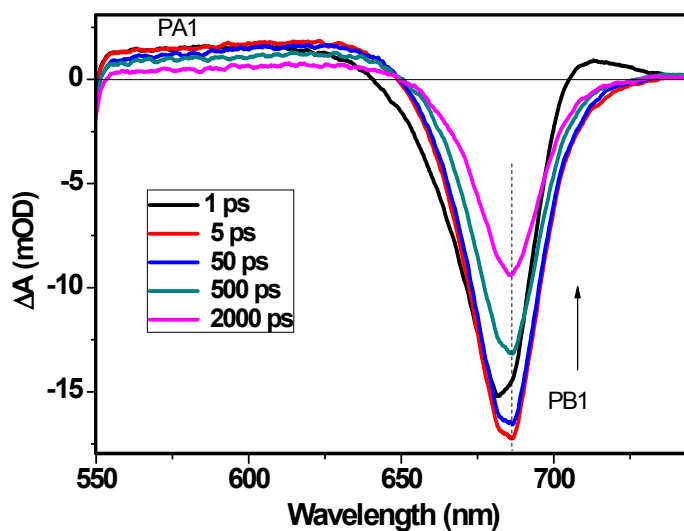


Figure S4. TA spectrum of CsPbI₃ NCs at 545 nm excitation.

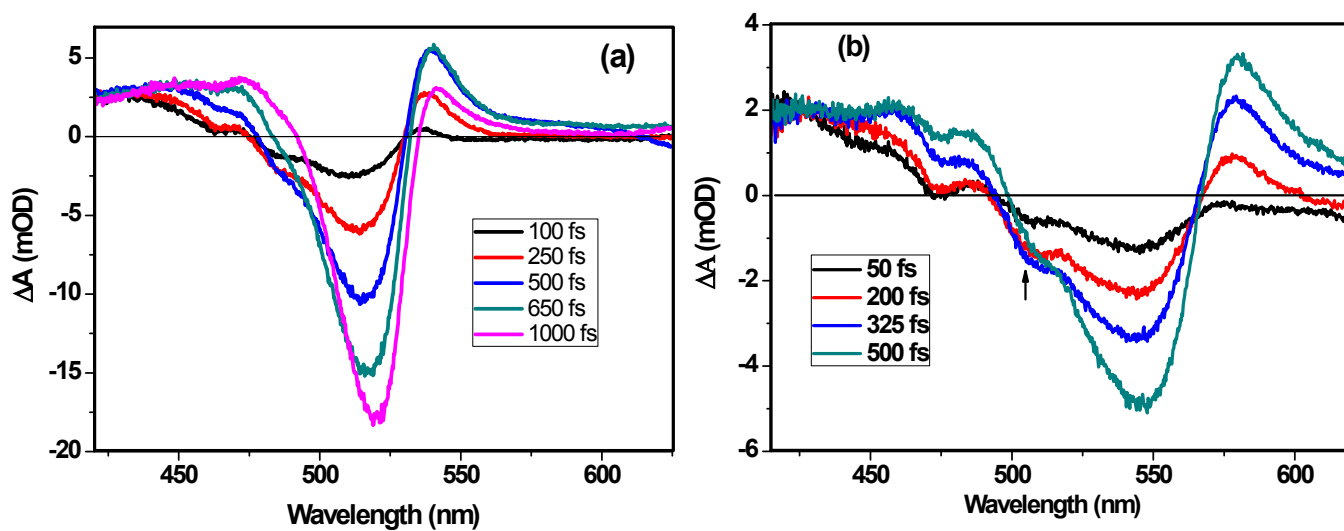


Figure S5. TA spectrum obtained on 350 nm excitation at shorter delay times for (a) CsPbBr₂I and (b) CsPbBr_{1.5}I_{1.5}.

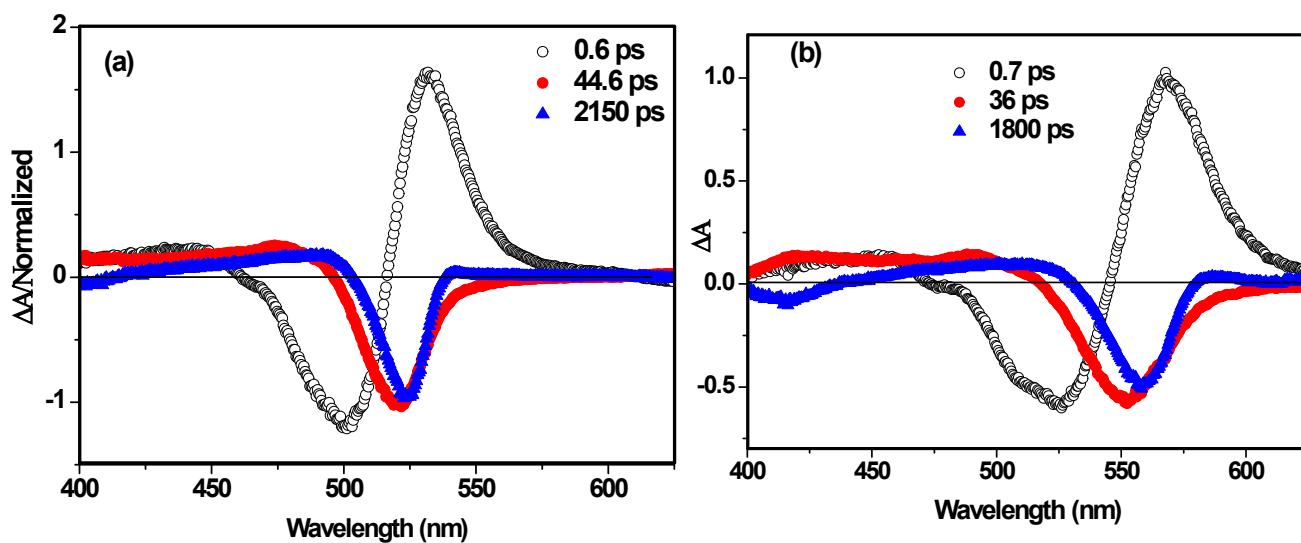


Figure S6. Decay associated spectrum ($\lambda_{\text{ex}} = 350$ nm) of (a) CsPbBr₂I and (b) CsPbBr_{1.5}I_{1.5} NCs.

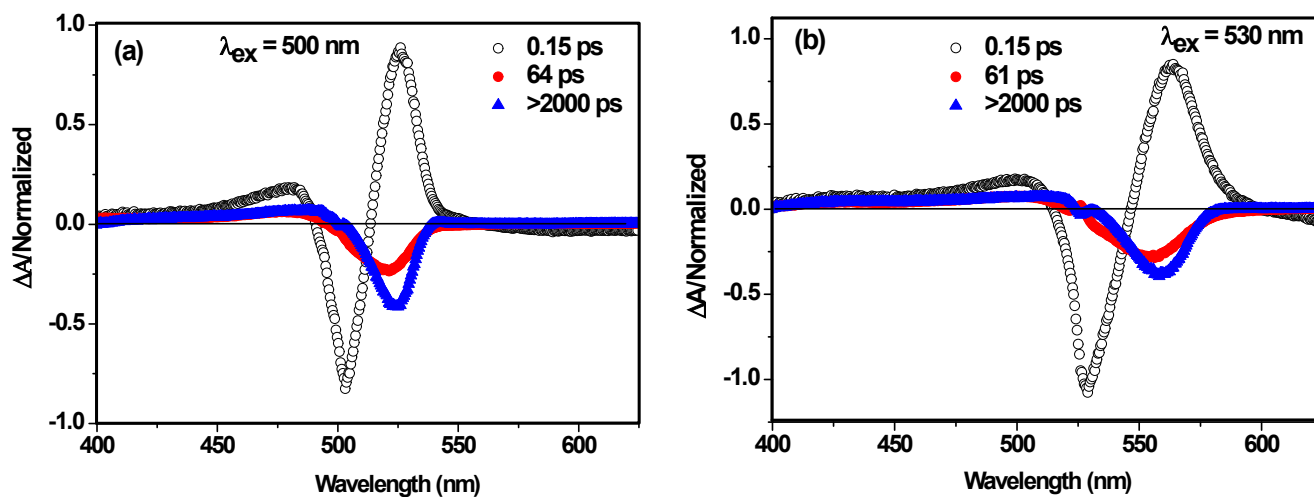


Figure S7. Decay associated spectrum of (a) CsPbBr₂I at 500 nm and (b) CsPbBr_{1.5}I_{1.5} at 530 nm excitation.

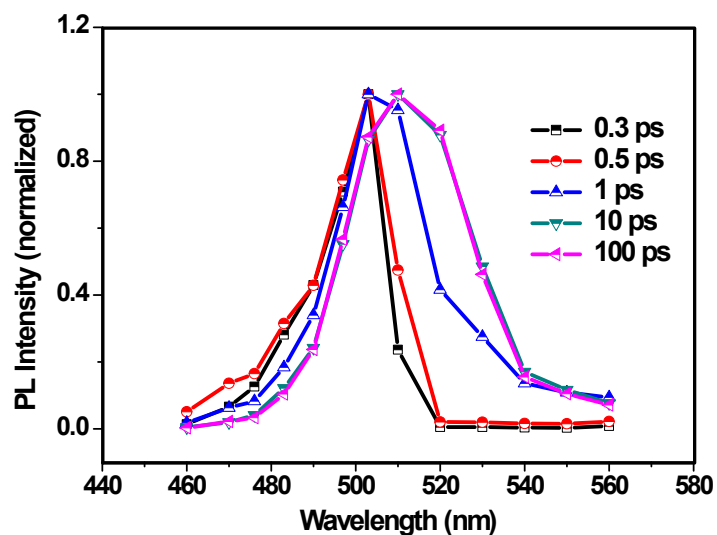


Figure S8. Normalized PL spectra of CsPbBr₃ NCs at different delay times

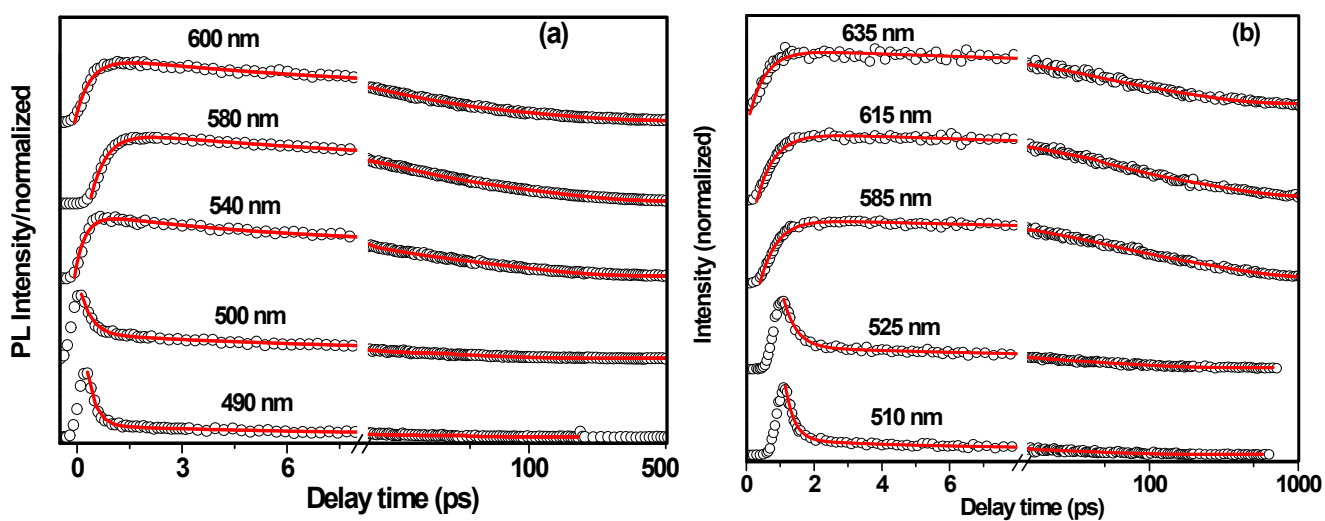


Figure S9. Up-converted PL ($\lambda_{\text{ex}} = 400$ nm) decay profiles monitored at (a) (490-600) nm for CsPbBr₂I and (b) (510-635) nm for CsPbBr_{1.5}I_{1.5}.

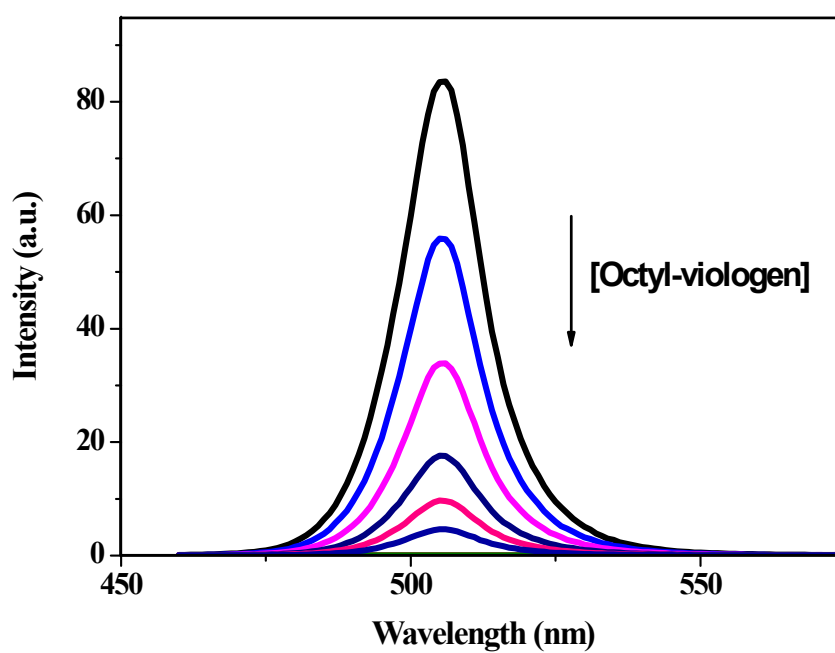


Figure S10. PL spectra ($\lambda_{\text{ex}} = 450 \text{ nm}$) of the NCs as a function of the concentration of OV (0, 33, 65, 98, 130, 160 μM).

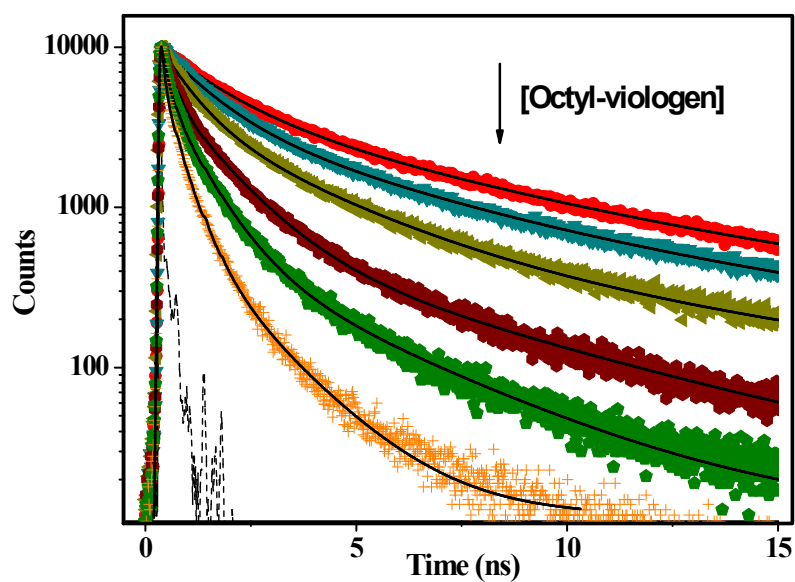


Figure S11. PL decay profiles of CsPbBr_3 NCs monitored at 510 nm in presence of different concentrations of OV (0, 33, 65, 98, 130, 160 μM). Black dashed line shows instrument response function.

Table S1. PL decay parameters for all three NCs monitored at their respective PL maximum.

Sample	$\tau_1(a_1)$ [ns]	$\tau_2(a_2)$ [ns]	$\tau_3(a_3)$ [ns]	$\langle\tau_{amp}\rangle^{\ddagger}$ [ns]
CsPbBr ₃	4.91 (0.44)	17.39 (0.38)	1.33 (0.18)	4.01
CsPbBr ₂ I	4.55 (0.14)	28.88 (0.82)	0.42 (0.03)	7.02
CsPbBr _{1.5} I _{1.5}	10.1 (0.12)	70.20 (0.86)	0.72 (0.02)	17.28
CsPbI ₃	30.76 (0.36)	102.87 (0.61)	5.80 (0.03)	55.90

$$\langle\tau_{amp}\rangle^{\ddagger} = (a_1\tau_1 + a_2\tau_2 + a_3\tau_3) / (a_1 + a_2 + a_3), \quad \langle\tau\rangle^{\ddagger} = \pm 5\%$$

Table S2. Bleach recovery kinetics for CsPbI₃ NCs at three different excitation wavelengths

λ_{pump} (nm)	λ_{probe} (nm)	$\tau_1(a_1)$ [ps]	$\tau_2(a_2)$ [ps]
545	585	218 ± 31 (0.20)	>2000 (0.80)
575	585	230 ± 61 (0.12)	>2000 (0.88)
635	585	----	>2000 (1.00)

Table S3. PL decay parameters for the CsPbBr₃ NCs monitored at 510 nm in absence and presence of different concentrations of OV.

[Octyl-viologen] (μM)	$\tau_1(a_1)$ [ns]	$\tau_2(a_2)$ [ns]	$\tau_3(a_3)$ [ns]	$\langle\tau_{int}\rangle$ (ns)
0	4.91 (0.44)	17.39 (0.38)	1.33 (0.18)	9.04
33.1	4.26 (0.43)	16.88 (0.35)	1.10 (0.22)	8.01
65.8	2.79 (0.44)	11.94 (0.33)	0.72 (0.22)	5.35
98.0	1.19 (0.51)	5.53 (0.33)	0.20 (0.16)	2.45
129.9	0.79 (0.51)	3.44 (0.29)	0.13 (0.20)	1.41
161.3	0.42 (0.46)	1.54 (0.27)	0.07 (0.28)	0.63

$$\langle\tau_{int}\rangle \text{ is defined as } \langle\tau_{int}\rangle = (a_1\tau_1^2 + a_2\tau_2^2 + a_3\tau_3^2) / (a_1\tau_1 + a_2\tau_2 + a_3\tau_3), \quad \langle\tau\rangle = \pm 5\%$$

Table S4. Up-converted PL ($\lambda_{\text{ex}} = 400$ nm) decay parameters for CsPbBr₃ NCs monitored at (470-550) nm

Sample	Monitoring wavelength (nm)	$\tau_1(a_1)$ /ps	$\tau_2(a_2)$ /ps	$\tau_3(a_3)$ /ps
CsPbBr ₃	550	0.40±0.02 (-1)	32.5±2.1 (0.58)	179±35 (0.42)
	510	0.44±0.008 (-1)	41.0± 1.9 (0.49)	290±25 (0.51)
	485	0.45±0.05 (0.23)	20.7±2.1 (0.35)	126±9 (0.42)
	475	0.33±0.01 (0.77)	19.0±3.2 (0.11)	116±19 (0.12)
	470	0.32±0.01 (0.76)	9.2±1.4 (0.08)	96±8.4 (0.16)

Table S5. Up-converted PL ($\lambda_{\text{ex}} = 400$ nm) decay parameters monitored at 510 nm for CsPbBr₃ NCs in presence of different concentrations of OV.

Quencher	Growth component	Decay components	
[Octyl-viologen]/mM	$\tau_1(a_1)$ /ps	$\tau_2(a_2)$ /ps	$\tau_3(a_3)$ /ps
0	0.40±0.02 (-1)	41.8±4.9 (0.49)	195±10.7 (0.51)
0.125	0.44±0.01 (-1)	23.6±1.2 (0.52)	87.4±5.6 (0.48)
0.250	0.40±0.05 (-1)	23.4± 0.8 (0.68)	95±8.6 (0.32)
0.375	0.45±0.05 (-1)	13.1±1.0 (0.63)	29.8±4 (0.37)
0.562	0.42±0.01 (-1)	6.1±0.40 (0.68)	14±2.2 (0.32)

Table S6. Up-converted PL ($\lambda_{\text{ex}} = 400$ nm) decay parameters for CsPbBr₂I NCs monitored at (490-600) nm.

Sample	Monitoring wavelength (nm)	$\tau_1(a_1)$ /ps	$\tau_2(a_2)$ /ps	$\tau_3(a_3)$ /ps
CsPbBr ₂ I	600	0.43±0.04 (-1)	19.9±3.4 (0.46)	162±28 (0.54)
	580	0.47±0.03 (-1)	29.2±2.9 (0.53)	239±36 (0.47)
	540	0.46±0.01 (-1)	33± 1.8 (0.47)	257±17 (0.53)
	500	0.58±0.04 (0.56)	8.1±1.3 (0.16)	83.6±7 (0.28)
	490	0.28±0.01 (0.62)	3.5±0.6 (0.19)	39.2±6 (0.19)

Table S7. Up-converted PL ($\lambda_{\text{ex}} = 400$ nm) decay parameters for CsPbBr_{1.5}I_{1.5} NCs monitored at (510-635) nm.

Sample	Monitoring wavelength (nm)	$\tau_1(a_1)$ /ps	$\tau_2(a_2)$ /ps	$\tau_3(a_3)$ /ps
CsPbBr _{1.5} I _{1.5}	635	0.50±0.04 (-1)	29.3±4.7 (0.47)	179±35 (0.53)
	615	0.53±0.02 (-1)	39.0±3.1 (0.51)	273±33 (0.49)
	585	0.50±0.02 (-1)	41.2± 2.8 (0.47)	290±25 (0.53)
	525	0.38±0.02 (0.72)	9.0±1.4 (0.13)	70±10 (0.15)
	510	0.27±0.01 (0.74)	3.3±0.5 (0.13)	38.8±5 (0.13)